Eur. Phys. J. D **15**, 47–56 (2001)

**THE EUROPEAN PHYSICAL JOURNAL D**

EDP Sciences


# Isotope dependent predissociation in the $C^1\Sigma^+$, v = 0 and v = 1 states of CO

P. Cacciani[1], F. Brandi[2], I. Velchev[2], C. Lyngå[3], C.-G. Wahlström[3], and W. Ubachs[2,a]

[1] Laboratoire PhLAM, Université des Sciences et Technologies de Lille, 59655 Villeneuve d'Ascq, France
[2] Department of Physics and Astronomy, Laser Centre Vrije Universiteit, De Boelelaan 1081, 1081 HV Amsterdam, The Netherlands
[3] Department of Physics, Lund Institute of Technology, P.O. Box 118, 22100 Lund, Sweden

Received 21 December 2000 and Received in final form 26 March 2001

**Abstract.** Rotationally resolved spectral lines in the $C-X(1,0)$ band of carbon monoxide are investigated under high resolution using a coherent vacuum ultraviolet laser source, continuously tunable near 107 nm. Transition frequencies are determined by calibrating against a reference standard of iodine lines, recorded with saturation spectroscopy in the visible range, yielding an absolute accuracy of 0.003 $cm^{-1}$ in the vacuum ultraviolet. Improved molecular constants for the excited state are derived and no effects of perturbation are found at the present level of accuracy. Line broadening measurements result in information on the excited state lifetime of the $C^1\Sigma^+, v = 1$ state for five natural isotopomers of carbon monoxide: $\tau(^{12}C^{17}O) = 280$ ps, $\tau(^{12}C^{18}O) = 210$ ps, $\tau(^{13}C^{16}O) = 295$ ps, $\tau(^{13}C^{17}O) = 160$ ps, and $\tau(^{13}C^{18}O) = 150$ ps. Within the accuracy of the present measurements no effects of $J$-dependent lifetimes were observed, for neither of the isotopomers. In addition direct time domain measurements of the lifetime of the $C^1\Sigma^+, v = 0$ and $v = 1$ states of the main isotopomer are performed in a pump-probe experiment using a picosecond VUV-laser, yielding $\tau(^{12}C^{16}O) = 1780$ ps for $v = 0$ and $\tau(^{12}C^{16}O) = 625$ ps for $v = 1$. For $C^1\Sigma^+, v = 0$ in $^{12}C^{16}O$ and $^{13}C^{16}O$ the same lifetime is found; this lifetime matches experimental values of the oscillator strength and hence supports previous results showing pure radiative decay in this state; the error margins however do not exclude some low level of predissociation. The measurements indicate that the $C^1\Sigma^+, v = 0$ state of the $^{13}C^{18}O$ isotopomer is predissociated with an estimated yield of 17% (*i.e.* above the level of predissociation for $^{12}C^{16}O$.) From the combined data predissociation yields upon excitation of the $C^1\Sigma^+, v = 1$ state are derived, lying in the range 0.84–0.91 for the five less abundant isotopomers; for the main $^{12}C^{16}O$ isotopomer a strongly deviating predissociation yield of 0.65 is deduced.

**PACS.** 33.20.Ni Vacuum ultraviolet spectra – 33.80.Gj Diffuse spectra; predissociation, photodissociation

## 1 Introduction

The $C-X$ system is a very intense feature in the absorption spectrum of the carbon monoxide molecule. Since the early works of Hopfield and Birge [1] and Tilford *et al.* [2] the vacuum ultraviolet (VUV) absorption in the $C-X$ system has also been investigated by Eidelsberg and Rostas [3], using a 10.5-m high-resolution spectrograph. Drabbels *et al.* [4] used two-photon induced fluorescence, whereas Ubachs *et al.* [5] employed a VUV laser source as well as 2+1 resonance enhanced multi-photon ionization. The $C^1\Sigma^+, v = 0$ level was observed in various infrared and visible emission studies as well [6–9].

The present study, focusing on the spectroscopy and predissociation dynamics of the $C^1\Sigma^+, v = 1$ level, was conducted in view of the astrophysical importance of the photodecomposition of CO by VUV-light. The photon-induced destruction of CO, the second most abundant molecule in outer space, has been shown to be a key parameter in the chemical dynamics of interstellar clouds [10]. The work of Letzelter *et al.* [11] has revealed, after suggestion by Bally and Langer [12], that the photodissociation proceeds *via* the mechanism of *pre*-dissociation rather than *via* continuum absorption.

The photo-predissociation is also largely responsible for the isotopic fractionation of CO in interstellar clouds. Such phenomena occurring as a function of penetration depths towards the centre of molecular clouds, relate to shielding effects on strong absorption features, as extensively discussed in the astrophysical literature (see *e.g.* [10,12]). In this respect particularly the $E^1\Pi, v = 0$ and $v = 1$ and the $C^1\Sigma^+, v = 1$ states are of importance because the predissociation yield is well below the 99% level found for higher lying states [3]; hence for these states there is a delicate competition between radiative and dissociative decay, whereas $C^1\Sigma^+, v = 0$ has hitherto been found to be unpredissociated. In the work by the Meudon group a zero predissociation yield is derived

[a] e-mail: wimu@nat.vu.nl

for $C^1\Sigma^+, v = 0$ from simultaneous measurements of absorption and fluorescence [3,11]. In the review by Morton and Noreau [13] the findings on lifetimes from a number of studies are compared to measurements of the oscillator strengths in the $C-X$ system; although there is some spread in the experimental values, they are generally in agreement with the assumption of pure radiative decay of the $C^1\Sigma^+, v = 0$ state.

Recently we reported on isotope dependent predissociation in the $E^1\Pi, v = 1$ state [14]. Here we report that also the predissociation in the $C^1\Sigma^+, v = 1$ state is also strongly dependent on the isotopic composition; but in this case the predissociation rates of the heavier isotopomers appear to be larger, in contrast to the case of the $E^1\Pi$, $v = 1$ state. As for the spectroscopic results of the present investigation the obtained line positions in the $C-X(1,0)$ band for $^{12}C^{16}O$, $^{12}C^{18}O$, $^{13}C^{16}O$, and $^{13}C^{18}O$ are an order of magnitude more accurate than the ones listed in a recent review compilation [13], while data for $^{12}C^{17}O$ and $^{13}C^{17}O$ are obtained for the first time.

## 2 Experimental

The narrow-band VUV laser setup of the Laser Centre Vrije Universiteit Amsterdam, based on a pulsed dye amplifier (PDA) system, has been described in detail in a previous publication [15]. Its application to the spectroscopy and predissociation of CO was documented recently for a similar investigation on the $E^1\Pi$, $v = 1$ state [16]. CO spectra were recorded by 1 VUV + 1 UV photoionization and a time-of-flight mass-separation and ion detection scheme were applied to investigate spectral features of the six natural isotopomers of the CO molecule: $^{12}C^{16}O$, $^{12}C^{17}O$, $^{12}C^{18}O$, $^{13}C^{16}O$, $^{13}C^{17}O$, and $^{13}C^{18}O$. Natural CO and a $^{13}C$ enriched sample (containing 99.15% $^{13}C$, 0.58% $^{17}O$ and 10.23% $^{18}O$) were used. The transition frequencies in CO were calibrated against a recently established dense grid of iodine molecular resonances by using the cw-output of a ring-dye-laser in saturation spectroscopy [17]. The VUV-light is produced by pulsed amplification of the cw-output of a ring-dye-laser near 640 nm and by subsequent frequency doubling and tripling of the pulsed output. The calibration procedure itself yields an absolute accuracy of the CO resonances of 0.001 $cm^{-1}$; however, chirp effects in the dye laser amplifier may cause net frequency shifts of the entire set of data by an amount less than 0.003 $cm^{-1}$ [18,19].

The isotope-dependent predissociation in the various isotopomers in the present study is inferred from line broadening measurements in a crossed molecular/laser beam study. Of crucial importance is the assessment of the instrument width in the measurement setup. The distance between the opening orifice of the pulsed valve producing the CO molecular beam and the skimmer was in most experiments taken at 4 cm. This configuration results in a very small contribution of Doppler broadening to the instrument linewidth. A series of measurements of linewidths on CO resonances was performed, with variation of the nozzle-skimmer distance and with variation of the gas composition in the probe-gas molecular beam. Close to the resonance wavelength of the $C-X(1,0)$ band of CO are also transitions in the $B-X(3,0)$ Lyman band of molecular hydrogen as well as resonances in xenon. Linewidths were deduced for pulsed beams of pure CO, Xe and $H_2$, as well as for mixtures of these gases. These measurements were used to unravel the Doppler contribution as well as the linewidth of the VUV-laser source.

A comparison was made with an alternative measurement of the lifetime of the $C^1\Sigma^+, v = 1$ excited state performed with a picosecond pump-probe laser system. These specific measurements were conducted at the Lund Laser Centre. The experimental setup and the general methods were described in reference [14]. The VUV-radiation used for excitation is produced by direct seventh harmonic generation of tunable infrared pulses. The duration of the laser pulses at the fundamental wavelength are 50–70 ps, resulting in somewhat shorter pulses in the VUV. A second UV-laser of 60 ps duration is used for ionization in a 1 VUV + 1 UV photoionization scheme. The temporal resolution is estimated to be 80 ps. The bandwidth of this source ($\approx 25$ $cm^{-1}$) is such, that no individual rotational levels can be excited.

## 3 Results and analysis

### 3.1 Spectroscopy

A typical recording of a CO resonance line with the narrow band VUV laser source is shown in Figure 1 for the R(4) line in the $C-X(1,0)$ band of the $^{12}C^{16}O$ isotopomer. The entire spectrum consists of 1300 frequency steps of the cw-ring-dye laser with the resonance covering 80 data points over the FWHM-profile; in most cases the signal was averaged over 5 consecutive laser pulses in the spectral recordings. For this CO resonance an iodine line was found to be very close, facilitating in the absolute calibration of the transition frequency. The line centre of the CO-resonance was determined by fitting a Lorentzian curve to the observed profile; the separation to the $t$-hyperfine component of the P58(7-4) line, marked with an asterisk in the spectrum, was evaluated in terms of fringe spacings of an actively stabilized etalon with FSR = 148.9567 MHz. In this way all observed resonances in the $C-X(1,0)$ band for all isotopomers were calibrated with respect to such a $t$-hyperfine component pertaining to one of the rotational lines in the $B-X(7,4)$ band of molecular iodine. All $t$-components of the (7, 4) band are well documented and calibrated to within 1 MHz ($1\sigma$ uncertainty) through work in the Amsterdam laboratory [17]. In several instances the nearest usable $I_2$ resonance was over a hundred etalon fringes away from the CO resonance, thus complicating the absolute calibration. In those cases fast overview scans were obtained to estimate the integer number of markers between the $I_2$ and CO resonances. The transition frequency of the CO resonance was then determined in a second stage by accurately recording the $I_2$ and CO resonances separately and using the fringes of the locked etalon (see Ref. [17]) as absolute frequency markers.

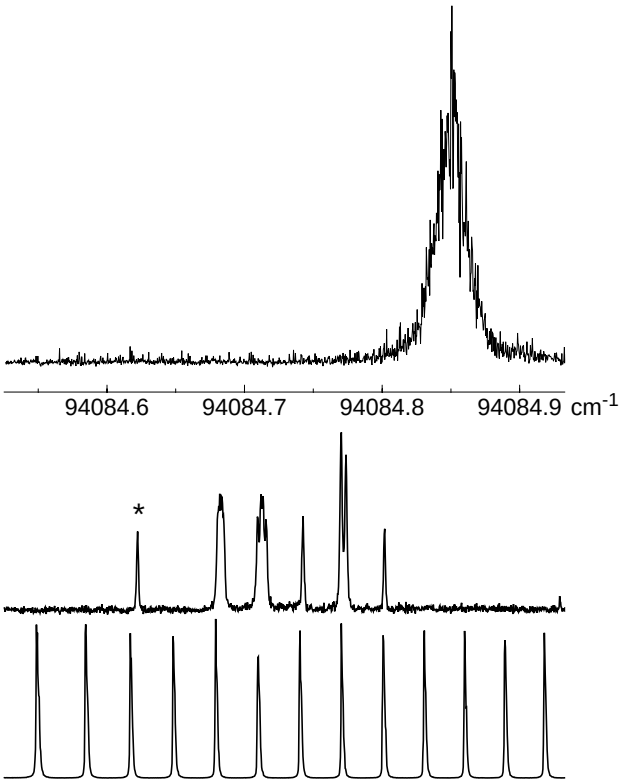


**Fig. 1.** Simultaneous recording of the R(4) resonance in the $C-X(1,0)$ band of $^{12}C^{16}O$ and the calibration spectra. In the upper panel the CO resonance, obtained from a beam of pure natural CO gas, is displayed on a frequency scale in the vacuum ultraviolet in $cm^{-1}$. The middle panel displays the spectrum recorded with saturation spectroscopy in $I_2$. The resonance marked with an asterisk is the $t$-component of the P58(7-4) line at 470097636.0 MHz. The lower panel represents the markers of an etalon (FSR = 148.9567 MHz) used in the calibration-interpolation procedure.

The obtained transition frequencies are listed in Tables 1–6 for the six natural isotopomers of CO. For the $^{17}O$ containing species, only present in low abundance in either the natural or the $^{13}C$ enriched gas samples, only a limited number of lines could be measured. The resonances were recorded at least two times and the estimated uncertainty in the determination of the transition frequency is 0.001 $cm^{-1}$. Also shown in Tables 1, 3, and 4, for the $^{12}C^{16}O$, $^{12}C^{18}O$, and $^{13}C^{16}O$ isotopomers are the data previously obtained by 1 VUV + 1 UV photoionization using a pulsed dye laser (PDL) as the fundamental light source; these hitherto unpublished data, marked with (a) in the tables, have an estimated accuracy of 0.04 $cm^{-1}$[5]. In cases, where values are available from studies with the PDL and the PDA systems, only the most accurate value was listed. The values in Tables 2, 5 and 6 are all obtained with the PDA-system.

The spectral data are analyzed in a least-squares fitting routine using a simple energy expression for the rotational levels of the excited state:

$$E(J) = \nu_{10} + BJ(J+1) - DJ^2(J+1)^2 \qquad (1)$$

**Table 1.** Transition frequencies in the $C-X(1,0)$ band of $^{12}C^{16}O$ and deviations from a least-squares fit. All values in $cm^{-1}$.

| | $R$-branch | | $P$-branch | |
|---|---|---|---|---|
| $J$ | frequency | $\Delta_{\mathrm{obs-calc}}$ | frequency | $\Delta_{\mathrm{obs-calc}}$ |
| 0 | 94069.451[a] | 0.016 | | |
| 1 | 94073.2862[b] | 0.001 | 94061.7419[b] | −0.001 |
| 2 | 94077.093[a] | −0.045 | 94057.9007[b] | 0.000 |
| 3 | 94080.9919[b] | 0.000 | 94054.057[a] | −0.004 |
| 4 | 94084.8490[b] | 0.000 | 94050.2244[b] | 0.000 |
| 5 | 94088.7052[b] | −0.002 | 94046.374[a] | −0.017 |
| 6 | 94092.5680[b] | −0.002 | 94042.5621[b] | 0.001 |
| 7 | 94096.459[a] | 0.031 | 94038.732[a] | −0.003 |
| 8 | 94100.302[a] | 0.011 | 94034.9116[b] | 0.000 |
| 9 | 94104.1547[b] | 0.000 | 94031.087[a] | −0.006 |
| 10 | 94108.0192[b] | 0.000 | 94027.2765[b] | −0.001 |
| 11 | 94111.8853[b] | 0.000 | 94023.480[a] | 0.014 |
| 12 | 94115.813[a] | 0.062 | 94019.6603[b] | 0.002 |
| 13 | 94119.625[a] | 0.007 | 94015.829[a] | −0.026 |
| 14 | 94123.542[a] | 0.057 | 94012.029[a] | −0.027 |
| 15 | 94127.411[a] | 0.060 | 94008.225[a] | −0.036 |
| 16 | 94131.238[a] | 0.020 | 94012.029[a] | −0.027 |
| 17 | 94135.117[a] | 0.033 | 94000.660[a] | −0.025 |
| 18 | 94138.995[a] | 0.045 | 93996.902[a] | −0.002 |
| 19 | 94142.877[a] | 0.062 | 93993.100[a] | −0.028 |
| 20 | 94146.705[a] | 0.027 | 93989.345[a] | −0.011 |
| 21 | 94150.623[a] | 0.082 | 93985.566[a] | −0.023 |
| 22 | 94154.467[a] | 0.065 | 93981.834[a] | 0.006 |
| 23 | 94158.297[a] | 0.036 | 93978.025[a] | −0.046 |
| 24 | 94162.115[a] | −0.003 | 93974.299[a] | −0.021 |
| 25 | 94165.958[a] | −0.016 | 93970.577[a] | 0.003 |
| 26 | 94169.816[a] | −0.010 | 93966.783[a] | −0.050 |
| 27 | 94173.753[a] | 0.076 | 93963.086[a] | −0.011 |
| 28 | | | 93959.340[a] | −0.026 |
| 29 | | | 93955.633[a] | −0.009 |
| 30 | | | 93951.884[a] | −0.038 |
| 31 | | | 93948.152[a] | −0.050 |

[a] Measured previously with PDL.
[b] Measured with the narrow-band PDA system.

**Table 2.** Transition frequencies in the $C-X(1,0)$ band of $^{12}C^{17}O$ and deviations from a least-squares fit. All values in $cm^{-1}$.

| | $R$-branch | | $P$-branch | |
|---|---|---|---|---|
| $J$ | frequency | $\Delta_{\mathrm{obs-calc}}$ | frequency | $\Delta_{\mathrm{obs-calc}}$ |
| 0 | 94042.2845 | −0.002 | | |
| 1 | 94046.0441 | 0.002 | 94034.7871 | 0.000 |
| 2 | 94049.7994 | −0.001 | | |

with $\nu_{10}$ the band origin and $B$ and $D$ the rotational constants. The rotational energy levels of the $X^1\Sigma^+, v = 0$ ground state for the various isotopomers were evaluated from the accurately determined constants by Guelachvili *et al.* [20] and kept fixed in the fitting routines. The values for the constants $B_0$, $D_0$ and $H_0$ derived from the

**Table 3.** Transition frequencies in the $C-X(1,0)$ band of $^{12}C^{18}O$ and deviations from a least-squares fit. All values in $cm^{-1}$.

| | $R$-branch | | $P$-branch | |
|---|---|---|---|---|
| $J$ | frequency | $\Delta_{obs-calc}$ | frequency | $\Delta_{obs-calc}$ |
| 0 | 94017.9571[b] | −0.002 | | |
| 1 | 94021.6299[b] | 0.000 | 94010.6323[b] | 0.002 |
| 2 | 94025.256[a] | −0.049 | 94007.077[a] | 0.103 |
| 3 | 94028.9846[b] | 0.001 | 94003.257[a] | −0.064 |
| 4 | 94032.635[a] | −0.032 | 93999.667[a] | −0.006 |
| 5 | 94036.355[b] | 0.002 | 93996.0304[b] | 0.000 |
| 6 | 94039.982[a] | −0.060 | 93992.373[a] | −0.020 |
| 7 | 94043.645[a] | −0.090 | 93988.758[a] | −0.002 |
| 8 | 94047.368[a] | −0.061 | 93985.090[a] | −0.042 |
| 9 | 94051.126[a] | −0.001 | | |
| 10 | 94054.815[a] | −0.011 | 93977.689[a] | −0.201 |
| 11 | 94058.479[a] | −0.047 | | |
| 13 | 94065.973[a] | 0.044 | | |

[a] Measured previously with PDL.
[b] Measured with the narrow-band PDA system.

**Table 4.** Transition frequencies in the $C-X(1,0)$ band of $^{13}C^{16}O$ and deviations from a least-squares fit. All values in $cm^{-1}$.

| | $R$-branch | | $P$-branch | |
|---|---|---|---|---|
| $J$ | frequency | $\Delta_{obs-calc}$ | frequency | $\Delta_{obs-calc}$ |
| 0 | 94022.149[a] | 0.031 | | |
| 1 | 94025.8022[b] | 0.000 | 94014.7585[b] | −0.003 |
| 2 | 94029.4933[b] | 0.002 | 94011.0918[b] | 0.002 |
| 3 | 94033.1839[b] | 0.000 | 94007.397[a] | −0.026 |
| 4 | 94036.8795[b] | 0.000 | 94003.737[a] | −0.024 |
| 5 | 94040.5810[b] | 0.001 | 94000.092[a] | −0.012 |
| 6 | 94044.2822[b] | −0.001 | | |
| 7 | 94047.973[a] | −0.017 | | |
| 8 | 94051.6994[b] | 0.000 | | |
| 9 | 94055.4114[b] | 0.000 | 93985.525[a] | −0.001 |
| 10 | 94059.227[a] | 0.101 | 93981.875[a] | −0.020 |
| 11 | 94062.910[a] | 0.067 | 93978.205[a] | −0.064 |
| 12 | 94066.597[a] | 0.034 | 93974.602[a] | −0.046 |
| 13 | 94070.321[a] | 0.037 | 93971.034[a] | 0.001 |
| 14 | 94073.989[a] | −0.017 | 93967.406[a] | −0.017 |
| 15 | 94077.724[a] | −0.006 | 93963.814[a] | −0.004 |
| 16 | | | 93960.196[a] | −0.023 |
| 17 | | | 93956.592[a] | −0.033 |
| 18 | | | 93953.025[a] | −0.012 |
| 19 | | | 93949.478[a] | 0.024 |
| 20 | | | 93945.884[a] | 0.007 |

[a] Measured previously with PDL.
[b] Measured with the narrow-band PDA system.

Dunham constants, listed by Guelachvili *et al.* [20], are given in reference [16].

The results of the weighted least-squares fits are presented in Table 7. It should be noted that the listed values for $\nu_{10}$ are the ones as obtained from the least-squares fits and thus relate to the internal consistency of the measurements. All listed uncertainties represent the $1\sigma$ standard deviation of the fits. The true uncertainty in $\nu_{10}$ is however

**Table 5.** Transition frequencies in the $C-X(1,0)$ band of $^{13}C^{17}O$ and deviations from a least-squares fit. All values in $cm^{-1}$.

| | $R$-branch | | $P$-branch | |
|---|---|---|---|---|
| $J$ | frequency | $\Delta_{obs-calc}$ | frequency | $\Delta_{obs-calc}$ |
| 0 | 93994.3341 | 0.002 | | |
| 1 | 93997.9188 | −0.003 | 93987.1696 | 0.001 |
| 2 | | | 93983.5905 | −0.005 |
| 3 | 94005.1218 | 0.005 | 93980.0297 | 0.002 |
| 5 | 94012.3284 | −0.002 | | |

**Table 6.** Transition frequencies in the $C-X(1,0)$ band of $^{13}C^{18}O$ and deviations from a least-squares fit. All values in $cm^{-1}$.

| | $R$-branch | | $P$-branch | |
|---|---|---|---|---|
| $J$ | frequency | $\Delta_{obs-calc}$ | frequency | $\Delta_{obs-calc}$ |
| 0 | 93969.4163 | 0.000 | | |
| 1 | 93972.9220 | 0.001 | 93962.4225 | −0.002 |
| 2 | 93976.4290 | −0.003 | | |
| 3 | 93979.9495 | 0.001 | 93955.4608 | 0.003 |
| 4 | 93983.4690 | −0.001 | | |
| 5 | 93986.9970 | 0.000 | 93948.5186 | 0.002 |
| 6 | | | 93945.0540 | −0.002 |
| 8 | 93997.6088 | 0.000 | 93938.1572 | 0.002 |
| 12 | 94011.8252 | 0.000 | | |

**Table 7.** Molecular constants for the $C^1\Sigma^+, v = 1$ state as obtained form least-squares fits to the data and derived ($1\sigma$ uncertainties). All values in $cm^{-1}$.

| | $\nu_{10}$ | $B$ | $D \times 10^6$ |
|---|---|---|---|
| $^{12}C^{16}O$ | 94065.5876(5) | 1.92383(1) | 6.25(3) |
| $^{12}C^{17}O$ | 94038.535(2) | 1.87584(22) | 6.0[f] |
| $^{12}C^{18}O$ | 94014.293(1) | 1.83324(8) | 6.5(8) |
| $^{13}C^{16}O$ | 94018.437(1) | 1.84017(3) | 6.0(2) |
| $^{13}C^{17}O$ | 93990.747(3) | 1.79217(20) | 6.0[f] |
| $^{13}C^{18}O$ | 93965.917(1) | 1.74946(5) | 5.4(3) |

[f] Value kept fixed in the fit.

estimated at 0.003 $cm^{-1}$because of possible chirp-induced effects in the dye amplifier [18,19].

A common energy reference for the $C^1\Sigma^+, v = 1$ levels of all isotopomers can be given with respect to the bottom of the potential well and to the dissociation limit. This can be achieved considering the zero point energy of the $X^1\Sigma^+$ state for each isotopomer, the dissociation limit $D_e = 90674 \pm 15\ cm^{-1}$ above the $X^1\Sigma^+$ ground state potential minimum derived in reference [21] and the energy of the bottom of the $C$ potential $E_C = 91916\ cm^{-1}$. This last value has been calculated in a Dunham analysis of the $C$ state including vibrational levels $v = 0$ to $v = 3$ of the different isotopomers [3,5]. Table 8 summarizes these values for the six different isotopomers. In the three rightmost columns the $C^1\Sigma^+, v = 1$ level energies

**Table 8.** $C^1\Sigma^+, v = 1$ level energies in wavenumber units.

| | mass[a] | $G_0(X)$[b] | $E_C(X)$[c] | $E_C(C)$[d] | $E_C(D)$[e] |
|---|---|---|---|---|---|
| $^{12}C^{16}O$ | 6.8562 | 1081.59 | 95147.17 | 3231 | 4473 |
| $^{12}C^{17}O$ | 7.0343 | 1067.85 | 95106.38 | 3190 | 4432 |
| $^{12}C^{18}O$ | 7.1999 | 1055.54 | 95069.83 | 3154 | 4395 |
| $^{13}C^{16}O$ | 7.1724 | 1057.55 | 95075.98 | 3160 | 4401 |
| $^{13}C^{17}O$ | 7.3676 | 1043.49 | 95034.23 | 3118 | 4360 |
| $^{13}C^{18}O$ | 7.5494 | 1030.88 | 94996.80 | 3081 | 4322 |

[a]Reduced mass of the isotopomer in a.u.
[b]Zero point vibration in the $X^1\Sigma^+$-well.
[c]Energy with respect to bottom of the $X^1\Sigma^+$ potential.
[d]Energy with respect to bottom of the $C^1\Sigma^+$ potential.
[e]Energy above dissociation limit.

are given above the $X^1\Sigma^+$ ground state potential minimum ($E_C(X)$), above the bottom of the $C$ state potential ($E_C(C)$), and above the C($^3$P) + O($^3$P) dissociation limit ($E_C(D)$).

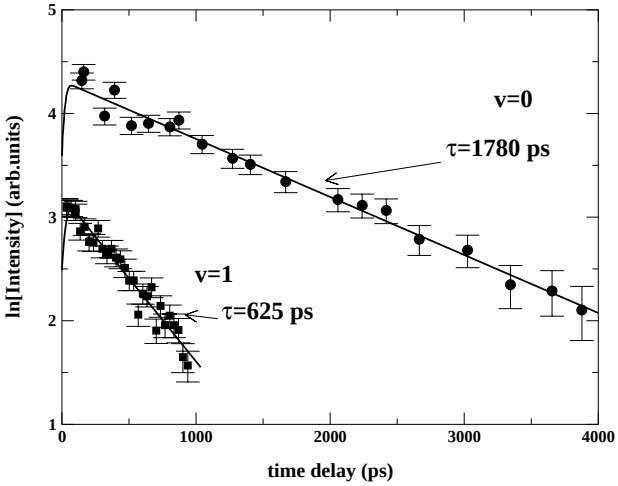


**Fig. 2.** Measurement of the pump-probe decay transient with the picosecond VUV-laser set at the unresolved $C-X(0,0)$ and $C-X(1,0)$ bands. Both measurements pertain to the $^{12}C^{16}O$ isotopomer.

### 3.2 Lifetimes and predissociation

Excited state lifetimes of the $C^1\Sigma^+$ state were determined both *via* time domain measurements and frequency domain line broadening experiments. These methods give complementary information and can be used to validate the results. The time domain pump-probe technique was applied to derive a lifetime for both the $C^1\Sigma^+, v = 0$ and $v = 1$ levels of the main $^{12}C^{16}O$ isotopomer, whereas line broadening experiments were performed on the $C^1\Sigma^+$, $v = 1$ state of all six natural isotopomers. The results will be presented in the following subsections.

#### 3.2.1 Time domain measurements

In Figure 2 the decay transients as obtained in a pump-probe experiment are displayed for the $C^1\Sigma^+, v = 0$ and $v = 1$ states of $^{12}C^{16}O$. The temporal scale on the horizontal axis in the figure represents the time delay between the VUV laser pulse, populating the $C^1\Sigma^+$ state, and the UV pulse that further transfers this population into the continuum; the ion signal is plotted as a function of temporal delay between the two laser pulses on a logarithmic scale. For all pump-probe lifetime measurements performed with the picosecond laser individual rotational states were not resolved and the cited results pertain to a set of quantum numbers in the range $J = 0-10$. The results are analyzed by deconvolution of the temporal response from the transients and by (weighted) fitting to an exponential decay. The uncertainties in the data points, as shown in Figure 2, include a Poisson noise component, scaling as the square-root of the intensity, and an electronic noise component which is constant. Some detail of the methods of analysis were described previously [14]. The large difference between the results, $\tau = 1.78 \pm 0.10$ ns for the $v = 0$ level and $\tau = 625 \pm 100$ ps for the $v = 1$ level, is an immediate consequence of the differing predissociation effects in these vibrational levels. The result pertaining to the lifetime of the $C^1\Sigma^+, v = 1$ state of $^{12}C^{16}O$ is used for the assessment of the natural lifetime broadening and the instrument function of the Amsterdam narrow-band VUV laser system.

For the $C^1\Sigma^+, v = 0$ state of the isotopomers $^{13}C^{16}O$ and $^{13}C^{18}O$ the time-domain measurements yield lifetimes of $1.77 \pm 0.10$ ns and $1.50 \pm 0.12$ ns. Time-delayed measurements, recorded simultaneously for the two species, are shown in Figure 3. This allows us to determine the difference between decay rates with good accuracy. Indeed intensity fluctuations of the XUV and the density fluctuations in the CO-beam, which are the main sources of error in the individual time delay signals, can be eliminated in the treatment by taking the ratio of the two simultaneously recorded signals for the two isotopomers considered. The total (dissociative + radiative) decay rates, defined as the inverse of the lifetime $\tau$, are $k_{\rm tot}(^{13}C^{16}O) = 5.7 \pm 0.3 \times 10^8$ s$^{-1}$, $k_{\rm tot}(^{13}C^{18}O) = 6.7 \pm 0.4 \times 10^8$ s$^{-1}$, when the separate transients are analyzed. The difference between the two decay rates, as obtained from analysis of the data in the lower panel of Figure 3 is $k_{\rm tot}(^{13}C^{18}O) - k_{\rm tot}(^{13}C^{16}O) = 1.2 \pm 0.3 \times 10^8$ s$^{-1}$. To address the predissociation in $^{13}C^{18}O$ for $C^1\Sigma^+, v = 0$ a few assumptions are made. Firstly, the $C^1\Sigma^+, v = 0$ state of $^{12}C^{16}O$ and $^{13}C^{16}O$ is considered to be unpredissociated. This is based on the experimental findings of the Meudon group [3,11], who report zero predissociation yield. Morton and Noreau [13] have argued that the observed lifetime of 1.78 ns would correspond to an oscillator strength of $f_{00} = 0.099$ if predissociation is neglected; this value matches, within the rather large uncertainties, a reliable experimental value for the oscillator strength $f_{00} = 0.117$ [22]. Then the radiative lifetime is taken as independent of isotopic constitution; this is an accepted assumption for non-hydride molecules. Based on these assumptions a common value of $5.6 \pm 0.2 \times 10^8$ s$^{-1}$

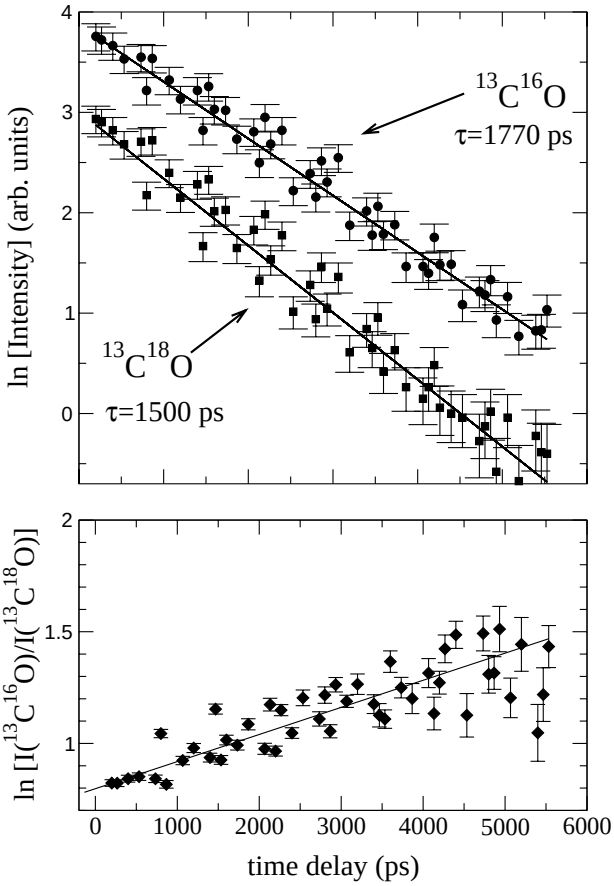


**Fig. 3.** Simultaneous lifetime measurement of the $C^1\Sigma^+, v = 0$ state of $^{13}C^{16}O$ and $^{13}C^{18}O$. In the lower panel the ratio between intensities clearly shows the difference in the decay rates.

for $k_{\rm rad}$ is adopted for both $^{12}C^{16}O$ and $^{13}C^{16}O$. From our measurements we then deduce a small dissociation rate of $1.2 \pm 0.3 \times 10^8\,{\rm s}^{-1}$ for the $^{13}C^{18}O$ species.

### 3.2.2 Line broadening measurements

Figure 4 shows a typical recording of broadened CO resonances obtained from a pure CO beam using a $^{13}C$ enriched sample. Two nearly coincident resonances are displayed, one in $^{13}C^{17}O$ and the other in $^{13}C^{18}O$, that have different widths. Throughout the study some variation in the linewidth is found for each isotopomer, but this was judged to be a statistical effect. No systematic trends were found as a function of rotational quantum number and in view of the limited signal-to-noise ratio (see *e.g.* Fig. 4) some spread is anticipated. Hence the observed linewidths for all rotational lines were averaged for each isotopomer. In Figure 5 the derived linewidths, fitted from the observed line profiles with Lorentzian functions, are displayed for three isotopomers: $^{12}C^{16}O$, $^{13}C^{16}O$, and $^{13}C^{18}O$. Here only a subset of data, recorded with a nozzle-skimmer distance of 4 cm, is included; hence the Doppler contribution to the widths in these measurements is equal. The spread in the main isotopomer $^{12}C^{16}O$ is

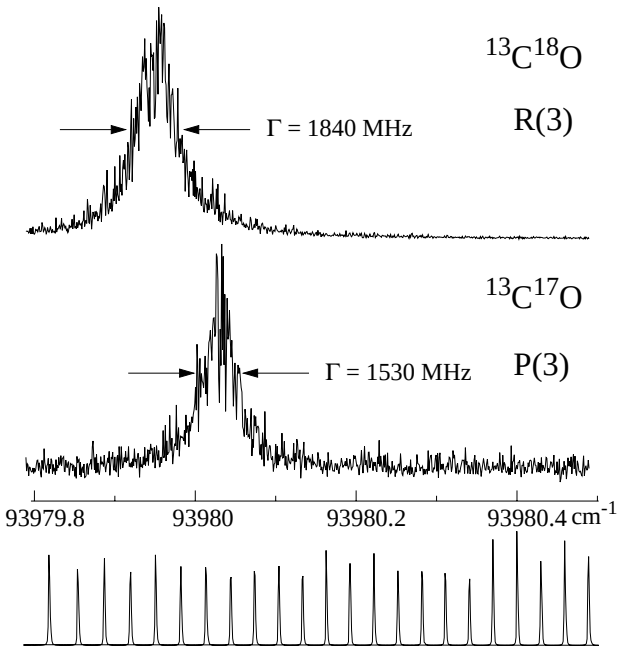


**Fig. 4.** Simultaneous recording of the R(3) resonance in $^{13}C^{18}O$ and the nearly lying P(3) resonance in $^{13}C^{17}O$ obtained from a $^{13}C$ enriched gas sample. Indicated is the observed linewidth.

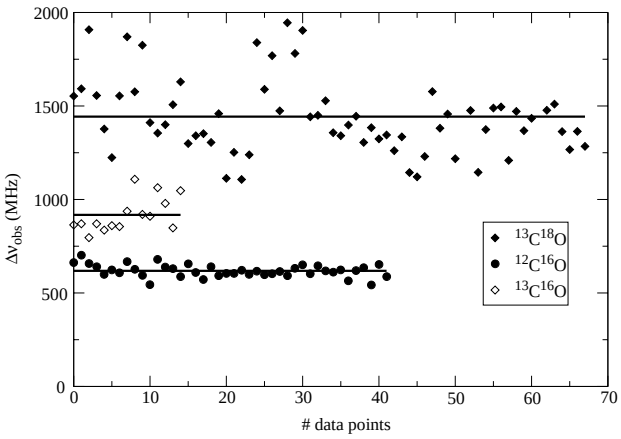


**Fig. 5.** Observed linewidths in the spectral recordings for three isotopomers.

much smaller than for the other ones. The average values for the line broadening parameters are given in Table 9, where the uncertainties represent a single standard deviation.

The resonances observed from pulsed molecular beams of pure CO could all be fitted to Lorentzian profiles. Even for the narrowest lines, obtained for $^{12}C^{16}O$, no evident contribution of a Gaussian component, representing the Doppler effect, could be discerned in the line profile for measurement conditions of 4 cm between nozzle and skimmer and for a pure CO beam. However, we have performed line broadening measurements using various resonance lines of atoms and molecules, having different

**Table 9.** Resulting widths as observed in line broadening experiments on the $C-X(1,0)$ band using the narrow-band VUV laser system. $\Gamma$ represents the intrinsic broadening due to the lifetime of the excited state obtained from the deconvolution procedure. The uncertainties in the value of $\Gamma$ are estimated at the level of 10–15%, except for the $^{12}C^{16}O$ isotopomer, for which the uncertainty is estimated at 30%. All values in MHz.

| | $\Delta\nu_{obs}$ | $\Gamma$ |
|---|---|---|
| $^{12}C^{16}O$ | 618 ± 5 | 225 |
| $^{12}C^{17}O$ | 923 ± 26 | 570 |
| $^{12}C^{18}O$ | 1137 ± 33 | 760 |
| $^{13}C^{16}O$ | 917 ± 22 | 540 |
| $^{13}C^{17}O$ | 1350 ± 80 | 980 |
| $^{13}C^{18}O$ | 1443 ± 24 | 1075 |

excited state lifetimes and velocities in the beam to further investigate this assumption.

From measurements on pulsed beams, containing 15% natural CO seeded in $H_2$, linewidths of 870 ± 50 MHz were obtained on $^{12}C^{16}O$ resonances. This is a clear indication that the instrument width in the crossed beam geometrical configuration is partially determined by the Doppler effect: the observed widths depend on the velocity of the molecules in the beam. Resonances in Xe and $H_2$ itself were also probed, under identical geometrical conditions. The $5p^6$–$5p^5 5d', k = 3/2, J = 1$ line in Xe at $\lambda = 107$ nm yields a linewidth of ≈ 350 MHz, whereas the $B-X(3,0)$R(0) line of $H_2$ yields a width of ≈ 1000 MHz.

The line broadening observed in the recording of the xenon spectral line (≈ 350 MHz) is taken as the bandwidth of the exciting laser radiation since for the low velocity beam of xenon Doppler broadening is negligible. The line profiles of the xenon resonances are close to Lorentzian shape; for this reason we assume that the VUV-laser bandwidth profile is of Lorentzian shape. From the molecular beam geometry used for the major part of the recordings a divergence of 20 mrad is estimated, which for a supersonically expanded beam of $H_2$ molecules would yield a Doppler width of 600 MHz. In view of the lifetime of the $B^1\Sigma_u^+, v = 3$ excited state of $H_2$ (500–700 ps) [24] and the bandwidth of ≈ 350 MHz this is consistent. The observed widths on the CO resonances of 870 MHz are a result of Doppler broadening due to the higher velocities in the seeded beam. If for the $H_2$ resonances a Doppler width contribution of 600 MHz is assumed, then for the case of a pure CO beam we derive a Doppler contribution of 160 MHz, from a comparison of estimated beam velocities in the expansion. This contribution is nearly negligible and a deviation from a Lorentzian profile on the CO resonances is not observed. Nevertheless we deconvolute this Gaussian contribution using the equation:

$$\Delta_L = \Delta_{obs} - \frac{(\Delta_G)^2}{\Delta_{obs}} \quad (2)$$

which is valid, under the present experimental conditions [25]. The instrument bandwidth $\Delta_{BW}$ of 350 MHz is then deconvoluted in a second step resulting in values for the natural lifetime broadening effect, represented by $\Gamma$ *via*

$$\Gamma = \Delta_L - \Delta_{BW} \quad (3)$$

which is the simple deconvolution of two Lorentzian functions. The resulting values of $\Gamma$ are listed in Table 9. Values for the excited state lifetime follow *via*

$$\tau = \frac{1}{2\pi\Gamma} \quad (4)$$

and are listed in Table 10. To emphasize the strong dependence of the decay rates on the isotopomer the values of $\Gamma$ are plotted as a function of reduced mass in Figure 6.

Except for the main isotopomer the uncertainty in the lifetime derives from line broadening and is estimated at 10–15%. For the main $^{12}C^{16}O$ isotopomer the lifetime-induced line broadening of 225 MHz, with a very small statistical error, is only marginally above the Doppler and bandwidth contributions. In view of the systematic uncertainties in these instrument parameters the error propagation results nevertheless in a large uncertainty in the value for the lifetime ($\tau = 700$ ps), which we estimate at 30%.

**Table 10.** Lifetimes $\tau$ of the $C^1\Sigma^+$ state of CO with uncertainties estimated at 10–15% (see text), and predissociation yield $\eta_{pre}$.

| | | $\tau$ (ps) | $\eta_{pre}$ |
|---|---|---|---|
| $C^1\Sigma^+, v = 1$ | $^{12}C^{16}O$ | 625 | 0.65[a] |
| | $^{12}C^{17}O$ | 280 | 0.84[b] |
| | $^{12}C^{18}O$ | 210 | 0.88[b] |
| | $^{13}C^{16}O$ | 295 | 0.83[b] |
| | $^{13}C^{17}O$ | 160 | 0.91[b] |
| | $^{13}C^{18}O$ | 150 | 0.91[b] |
| $C^1\Sigma^+, v = 0$ | $^{12}C^{16}O$ | 1780 | 0[a] |
| | $^{13}C^{16}O$ | 1770 | 0[a] |
| | $^{13}C^{18}O$ | 1500 | 0.17[a] |

[a] Value taken from time-domain measurements.
[b] Value taken from line broadening.

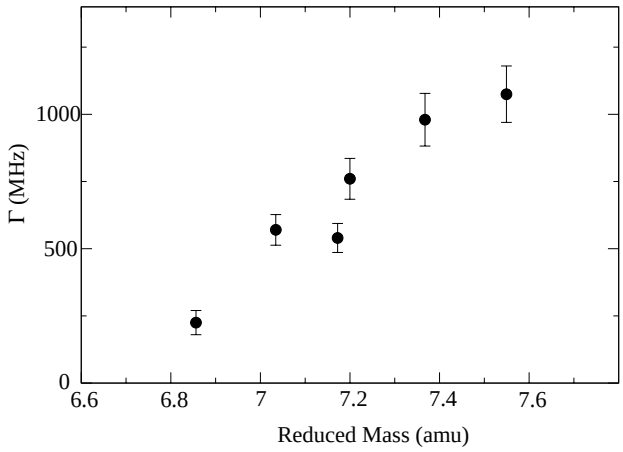


**Fig. 6.** Total decay rate $\Gamma$ (including radiative and predissociative decay) for the $C^1\Sigma^+, v = 1$ excited state as a function of reduced mass for the six CO isotopomers; data obtained from line broadening measurements.

The value for the lifetime of the $C^1\Sigma^+, v = 1$ state of $^{12}C^{16}O$, as determined in the time-domain experiment is 625 ps, with an estimated uncertainty of 100 ps. This result is more accurate than obtained from line broadening and sets in fact the error level for the lifetime in the main isotopomer at 15%; this value is included in the data set of Table 10. The direct time-domain value of 625 ps agrees well enough with the estimate from the line broadening and deconvolution procedure to tie the data sets in a convincing manner. It should be noted in conclusion that, although the derivation of lifetimes on an absolute scale gives somewhat large error margins, the trend in observed widths $\Delta\nu_{\rm obs}$ shows a distinct isotope dependence; the values listed in Table 9 were all obtained in the same geometrical configuration and for the same source bandwidth.

## 4 Discussion and conclusion

In the present study absolute transition frequencies of individual rotational lines in the $C-X(1,0)$ band of CO have been determined with unprecedented accuracy. While the value for the band origin $\nu_{10}$ for the main $^{12}C^{16}O$ isotopomer has an internal consistency of 0.0005 cm$^{-1}$, the uncertainty in the absolute transition frequency is 0.003 cm$^{-1}$ due to possible chirp-induced effects. Our value agrees well with the less accurate value listed in the recalibrated data-atlas by the Meudon-group [26]. For the $^{13}C^{16}O$ isotopomer the largest discrepancy is found: the atlas lists an internally consistent value in the Meudon data of 94018.55 cm$^{-1}$ with a $3\sigma$ uncertainty of 0.04 cm$^{-1}$; however, the absolute accuracy is only claimed to be within 0.1 cm$^{-1}$, in reasonable agreement with the present finding. For the $C-X(1,0)$ band a line list was produced in the review compilation by Morton and Noreau [13]. The presently derived molecular constants, in combination with the ground state constants of Guelachvili *et al.* [20] provide a basis to calculate an improved set of transition frequencies for all six natural isotopomers of CO. No perturbation of the rotational structure is found at the present level of accuracy and for the range of $J$-values observed.

Time-domain measurements yield a value for the lifetime of the $C^1\Sigma^+$, $v = 0$ state of $^{12}C^{16}O$ of $1.78 \pm 0.1$ ns. In the paper by Krishnakumar and Srivastava [23], and in the review by Morton and Noreau [13] five different measurements are discussed that give values in the range 1.1 to 2.2 ns, with a mean of $1.78 \pm 0.5$ ns, which is in excellent agreement with the present finding. For the $C^1\Sigma^+, v = 0$ state of $^{13}C^{16}O$ the same lifetime is found, while for the heavier $^{13}C^{18}O$ a small but significant deviation is obtained. With the assumption that the value of 1.78 ns corresponds to the radiative lifetime [3] it follows *via*

$$\eta_{\rm pre} = 1 - \frac{\tau}{\tau_{\rm rad}} \tag{5}$$

that the predissociation yield in $^{13}C^{18}O$ ($C, v = 0$) is 17%. We note again that the obtained value for the lifetime is in accordance with reported values for the oscillator strength [13,22]. But in view of the uncertainties in those values it cannot be excluded that the $C^1\Sigma^+, v = 0$ state of $^{12}C^{16}O$ and $^{13}C^{16}O$ is predissociated nonetheless. In such case the 17% predissociation yield for $^{13}C^{18}O$ is only a lower limit.

For the $C^1\Sigma^+, v = 1$ state no measurements are reported, other than the order-of-magnitude estimate by Eidelsberg and Rostas [3] of $10^{-9}$ s. In that paper a predissociation yield is given for the $C^1\Sigma^+, v = 1$ state: $\eta_{\rm pre} = 0.60$ for both $^{12}C^{16}O$ and $^{13}C^{16}O$. Again with the value of 1.78 ns representing the radiative lifetime for the $C^1\Sigma^+$ state, an observed lifetime of 625 ps corresponds to a dissociation yield of $\eta_{\rm pre} = 0.65$ for $^{12}C^{16}O$ ($C, v = 1$) in good agreement with the estimate of Eidelsberg and Rostas [3]. The derived values for the predissociation yields pertaining to the isotopomers are listed, along with the excited state lifetimes, in Table 10. Because of the propagation of errors the uncertainty in the value for $\eta_{\rm pre}$ for the main isotope is, with 10%, the largest. At the same time the isotopic effect in the predissociation yield comes out most strongly for the main $^{12}C^{16}O$ isotopomer. This effect, which is not included in current models, may have important consequences for the isotopic fractionation in interstellar space. An estimate with propagation of errors yields uncertainties of only 2% for $\eta_{\rm pre}$ of the other five isotopomers.

In a recent paper by Li *et al.* [27] an *ab initio* calculation of the predissociation rates in the $B^1\Sigma^+$ and $C^1\Sigma^+$ excited states is reported. For ease of reading we have included a picture with the relevant potential curves in Figure 7. In the adiabatic picture the $(3s\sigma)B^1\Sigma^+$ Rydberg state couples with the $(\pi^3\pi^*)D'^1\Sigma^+$ valence state to obey the non-crossing rule, forming a double well structure. In this picture the predissociation in the $B^1\Sigma^+$ state can be computed from intramolecular tunneling in this adiabatic double well structure. Using the alternative semi-empirical framework of close-coupling theory Tchang-Brillet *et al.* [28] were able to quantitatively reproduce predissociation rates and breaking off of emission progressions in the $B$ state. They showed that the first predissociation, setting in at $v_B = 0, J_B = 37$ and $v_B = 1, J_B = 17$, cannot be explained from $B-D'$ coupling; hence other states are responsible for predissociation in this energetic range as well.

According to Li *et al.* [27] the $(3p\sigma)C^1\Sigma^+$ Rydberg state similarly forms an adiabatic double well structure with the $C'^1\Sigma^+$ valence state arising from a $\pi^2\pi^{*2}$ molecular orbital configuration; the dissociation limit and the barrier of the resulting adiabatic potential are so high that tunneling cannot cause predissociation in the $C^1\Sigma^+$ state. The predissociation effect in the $C^1\Sigma^+$ state is ascribed to a non-adiabatic interaction with the $D'^1\Sigma^+$; this $D'^1\Sigma^+$ state is held responsible for predissociation in many Rydberg states, such as the $(4p\pi)L^1\Pi$ and the $(3s\sigma\, A^2\Pi)W^1\Pi$ states [25]. Rates of predissocation are computed yielding $k_{\rm p} = 10^{10}$ s$^{-1}$ for the $C^1\Sigma^+, v = 1$ level. Predissociation rates $k_{\rm p}$ for $v = 0{-}4$ as calculated in reference [27] are plotted in Figure 8 as a function of energy above the bottom of the $C$ state potential well.

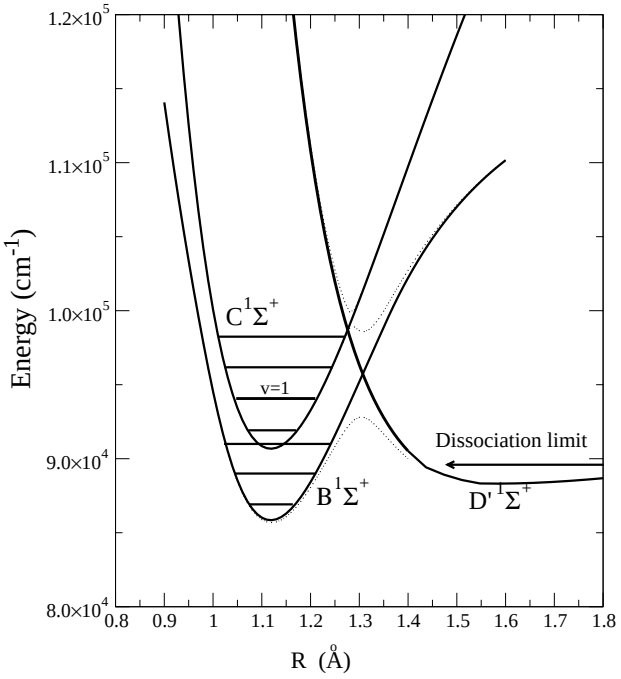


**Fig. 7.** Potential curves of relevance for the present experiment: full lines represent the diabatic curves for the $(3s\sigma)B^1\Sigma^+$, $(3p\sigma)C^1\Sigma^+$ and $(\pi^3\pi^*)D'^1\Sigma^+$ states, while the dotted curves represent adiabatic potentials.

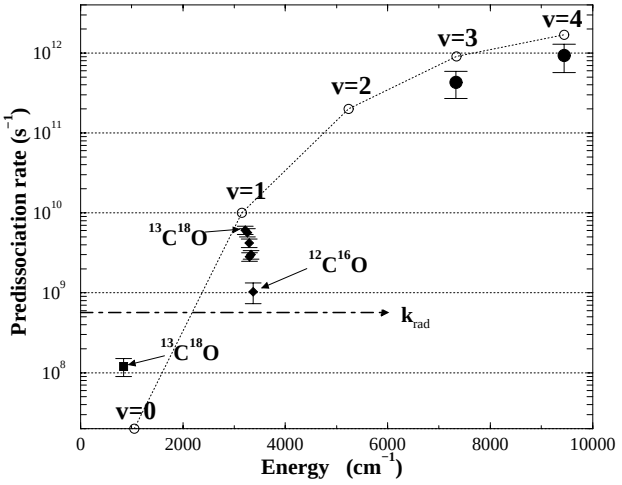


**Fig. 8.** Predissociative decay rate as a function of the excitation energy in the potential well of the $C$ state. Square: experimental data for $v = 0$; diamond: experimental data for $v = 1$; closed circles: experimental data as cited in reference [28]; open circles: calculation of reference [27]. The dashed line indicates the level of radiative decay.

The presently obtained experimental rates are calculated using $k_\mathrm{p} = \Gamma - k_\mathrm{rad}$ and a radiative decay rate $k_\mathrm{rad}$ of $5.6 \times 10^8$ s$^{-1}$, indicated also in Figure 8. Data for $C^1\Sigma^+, v = 3$ and $v = 4$ were obtained from reference [28] based on unpublished work by the Meudon group.

The theoretical investigation provides an explanation for the varying decay rates with vibrational quantum number although the value for $C, v = 1$ of the main isotopomer is off by a factor of seven from the present experimental value. The observed very strong mass-dependence of the predissociation rate indicates that there prevails a subtle dependency on the exact location of the potentials. In view of the non-adiabatic interaction mechanism no direct intuitive explanation can be given for these reduced mass effects, nor for the discrepancies found. The observation that the predissociation in the $C^1\Sigma^+$ state is independent on rotational quantum number gives some handle to identify the states causing the predissociation. A homogeneous perturbation can be produced by coupling to a state of the same symmetry ($^1\Sigma^+$), but also coupling with states of $^3\Sigma$ or $^3\Pi$ symmetry could produce such a behavior. It is noted that the $\pi^2\pi^{*2}$ molecular orbital configuration supports a state of $^3\Sigma^-$ symmetry. The present findings on the predissociation in the $C^1\Sigma^+, v = 1$ state of carbon monoxide may be taken as a challenge for future studies by theoretical chemists.

Financial support from the Foundation for Fundamental Research on Matter (FOM) is gratefully acknowledged. P.C. acknowledges support from the Dutch/French NWO/CNRS collaboration program. The data on the time domain lifetime measurements were obtained with the Lund Laser Centre picosecond laser system. The latter work was performed with support from the European Community *via* the TMR-grant "Access to Large Scale Facilities", contract ERBFMGECT950020(DG12). We thank A. L'Huillier (Lund) and K.P. Huber (Ottawa) for critically reading the manuscript and W.-Ü.L. Tchang-Brillet for fruitful discussions.

## References

1. J.J. Hopfield, R.T. Birge, Phys. Rev. **29**, 922 (1927).
2. S.G. Tilford, J.T. Vanderslice, P.G. Wilkinson, Can. J. Phys. **43**, 450 (1965).
3. M. Eidelsberg, F. Rostas, Astron. Astrophys. **235**, 472 (1990).
4. M. Drabbels, W.L. Meerts, J.J. ter Meulen, J. Chem. Phys. **99**, 2352 (1993).
5. W. Ubachs, P.C. Hinnen, P. Hansen, S. Stolte, W. Hogervorst, P. Cacciani, J. Mol. Spectr. **174**, 388 (1995).
6. C. Amiot, J.-Y. Roncin, J. Vergès, J. Phys. B **19**, L19 (1986).
7. J.-Y. Roncin, A. Ross, E. Boursey, J. Mol. Spectr. **162**, 353 (1993).
8. R. Kepa, Chem. Phys. **110**, 123 (1986).
9. R. Kepa, J. Mol. Spectr. **135**, 119 (1989).
10. E.F. van Dishoeck, J.H. Black, Astroph. J. **334**, 771 (1988).
11. C. Letzelter, M. Eidelsberg, F. Rostas, J. Breton, B. Thieblemont, Astron. Astrophys. **193**, 265 (1988).
12. J. Bally, W.D. Langer, Astroph. J. **255**, 143 (1982).
13. D.C. Morton, L. Noreau, Astroph. J. Suppl. Ser. **95**, 301 (1994).
14. P.C. Cacciani, W. Ubachs, P.C. Hinnen, C. Lyngå, A. L'Huillier, C.-G. Wahlström, Astroph. J. Lett. **499**, L223 (1998).

15. W. Ubachs, K.S.E. Eikema, W. Hogervorst, P.C. Cacciani, J. Opt. Soc. Am. B **14**, 2469 (1997).
16. W. Ubachs, I. Velchev, P. Cacciani, J. Chem. Phys. **113**, 547 (2000).
17. S.C. Xu, R. van Dierendonck, W. Hogervorst, W. Ubachs, J. Mol. Spectr. **201**, 256 (2000).
18. N. Melikechi, S. Gangopadhyay, E.E. Eyler, J. Opt. Soc. Am. B **11**, 2402 (1994).
19. K.S.E. Eikema, W. Ubachs, W. Vassen, W. Hogervorst, Phys. Rev. A **55** 1866 (1997).
20. G. Guelachvili, D. de Villeneuve, R. Farrenq, W. Urban, J. Vergès, J. Mol. Spectr. **98**, 64 (1983).
21. M. Eidelsberg, J.Y. Roncin, A. Le Floch, F. Launay, F. Rostas, J. Mol. Spectr. **121**, 309 (1987).
22. W.F. Chan, G. Cooper, C.E. Brion, Chem. Phys. **170**, 123 (1993).
23. E. Krishnakumar, S.K. Srivastava, Astroph. J. **307**, 795 (1986).
24. A. Pardo, Spectrochim. Acta A **54**, 1433 (1998).
25. K.S.E. Eikema, W. Hogervorst, W. Ubachs, Chem. Phys. **181**, 217 (1994).
26. M. Eidelsberg, J.J. Benayoun, Y. Viala, F. Rostas, P.L. Smith, K. Yoshino, G. Stark, C.A. Shettle, Astron. Astroph. **265**, 839 (1992).
27. Y. Li, R.J. Buenker, G. Hirsch, Theor. Chem. Acc. **100**, 112 (1998).
28. W.-Ü.L. Tchang-Brillet, P.S. Julienne, J.-M. Robbe, C. Letzelter, F. Rostas, J. Chem. Phys. **96**, 6735 (1992).